J. Plasma Physics (2013), *vol.* 79, *part* 1, *pp.* 55–64. © Cambridge University Press 2012
doi:10.1017/S0022377812000694

Effect of the inter-grain attractive potential on lattice dynamics in complex plasmas

M. P. VERMA[1], S. K. MISHRA[2] AND M. S. SODHA[1]

[1]Department of Education Building, University of Lucknow, Lucknow 226007, India
(msodha@rediffmail.com)
[2]Institute for Plasma Research, Gandhinagar 382428, India

(Received 28 May 2012; revised 27 June 2012; accepted 27 June 2012; first published online 20 August 2012)

Abstract. The dispersion relation for lattice waves in a linear chain of charged particles in a complex plasma has been derived on the basis of a screened inter-grain repulsive potential and an attractive shadow potential $1/r$. It is seen that the inclusion of the attractive potential makes a significant difference in the results; the present results are in good agreement with the experiment. The dispersion relations, corresponding to square and hexagonal planar lattices, with vibrations confined to the plane have also been derived.

1. Introduction

Ikezi (1986) suggested on theoretical grounds that dust grains suspended in plasmas could organize themselves in symmetric patterns (or a Coulomb lattice). Later, in 1994, five different groups experimentally observed such symmetric patterns (Chu and Lin 1994; Hayashi and Tachibara 1994; Melzer et al. 1994; Sato et al. 1994; Thomas et al. 1994; Homann et al. 1997), which presented three-dimensional (3D) *fcc* and *bcc* structures, 2D *square* and *hexagonal* structures and 1D linear chain structures; such structures were also theoretically predicted later by Vladimirov and Ishihara (1996). The grains have a size of the order of a few microns (1 μm to 10 μm), a separation between nearest neighbours $a \approx 300\,\mu$m and carry a charge as high as $-10^5 e$, where $-e$ is the electronic charge. The particles further acquire a steady-state charge in a very short time $\ll$1s. These features are amenable to direct observations and hence the grain structures are an ideal system for the study of lattices.

A number of experimental and theoretical studies (e.g. Pieper and Goree 1996; Quinn et al. 1996; Shukla and Mamun 2002; Mitie et al. 2008; Klumov et al. 2009; Morfill and Ivlev 2009; Nakamura and Ishihara 2009; Shukla and Eliasson 2009; Baruah and Das 2010) on the lattice formation in complex plasmas and corresponding structural analyses have been reported; properties like those of solids, liquids and gases viz. phase transition (Melandso 1997; Khrapak et al. 2006, 2007; Knapek et al. 2007; Avinash et al. 2009), inter-grain interactions (Resendes et al. 1998; Lampe et al. 2000; Khrapak et al. 2002, 2006, 2010; Kompaneets et al. 2007; Khrapak and Morfill 2008; Chaudhuri et al. 2010), lattice vibrations and dust lattice waves in 1D (Melandso 1996; Vladimirov et al. 1997; Ivlev and Morfill 2000; Misawa et al. 2001; Yaroshenko et al. 2005), 2D (Vladimirov et al. 1999, 2006; Bin Liu et al. 2009; Couëdel et al. 2009) and 3D (Pramanik et al. 2002; Antonova et al. 2008) lattices have been investigated.

In contrast to the usual analyses of lattice waves in complex plasmas, based on the fluid dynamical equations, the authors have followed the usual approach in conventional lattice dynamics, outlined in many books, e.g. by Born and Huang (1994) and Maradudin et al. (1971). The starting point for such investigations is an analysis of vibrations of atoms (in the present case, dust particles) in the lattice around their equilibrium positions. For this purpose, knowledge of the inter-grain potential $\varphi(r)$ is essential. In most of the studies the repulsive inter-grain electric potential energy $\varphi_R(r)$ in a complex plasma is represented by the Debye–Hückel (or Yukawa) potential, i.e.

$$\varphi_R(r) = \left(Z_d^2 e^2/r\right)\exp[-r/\lambda], \tag{1}$$

where $-Z_d e$ is the charge on the particle, $-e$ is the electronic charge and λ is the Debye screening length.

The above equation is obtained from the Poisson equation by the linearization of the Boltzmann distribution of electrons and ions. However, the numerical solution of the Poisson equation along with the exponential Boltzmann distribution of electrons/ions can, to a very good approximation, be represented by the Yukawa potential (Nefedov et al. 1998; Bystrenko and Zagardny 1999). Ratynskaia et al. (2006) have numerically evaluated $\varphi_R(r)$, taking into account ion-neutral collisions and collective effects, and concluded that $\varphi_R(r)$ can be represented by (1) with $\lambda = (1 + 0.2\beta^{1/2})\lambda_{D_i}$ where λ_{D_i} is the ion Debye screening length, $\beta(= Z_d e^2/k_B T_i \lambda_{D_i})$, T_i is the ion temperature and k_B is the Boltzmann constant.

It is instructive to note that for typical complex plasmas in the crystalline state, characterized by $Z_d = 10^4 - 10^5$, $T_i = 300$ K, $2 < (a/\lambda_{D_i}) < 4$ and $300 < a < 900\,\mu$m, the parameter $\beta(= Z_d e^2/k_B T_i \lambda)$ lies between

https://doi.org/10.1017/S0022377812000694 Published online by Cambridge University Press

1.23 and 75; here a is the equilibrium grain separation. These values may be seen in the context of a statement made by Tsytovich et al. (2008) that the condensation of complex plasmas occurs for β larger than 35.

Lampe et al. (2003) considered the effect of trapped ions and concluded that the numerical results fitted with the Yukawa potential (1) with $\lambda \approx (1 \text{ to } 2)\lambda_{D_i}$. Thus, there is a strong case for the use of the Yukawa potential (with λ as a function of λ_{D_i}) in complex plasma studies. The case is strengthened by direct experimental evidence (Konopka et al. 2000) for the Yukawa potential, although there are some doubts (Kompaneets et al. 2007) about the interpretation of the observations.

Tsytovich et al. (2008) have pointed out that for large values of β the linearized form of the Boltzmann distribution function and hence the Yukawa repulsive potential are not valid. These authors have accounted for the nonlinearity by assuming the repulsive potential to be proportional to $r^{-1}\psi(r)$; the r^{-1} term is just the Coulomb potential, while $\psi(r)$ arises from the nonlinearity in the inter-grain interaction. It was seen that to a very good approximation the repulsive potential $\varphi'_R(r)$ can be represented by

$$\varphi'_R(r) = \left(Z_d^2 e^2/r\right)(1 - r/\lambda_g)^4 \quad \text{for} \quad r < \lambda_g, \tag{2a}$$

$$\varphi'_R(r) = 0 \quad \text{for} \quad r > \lambda_g, \tag{2b}$$

where $\lambda_g = 3.4\lambda_{Di}(\pi\beta/4)^{1/5}$ is known as the Gurevich screening length (Tsytovich et al. 2004) and lies between 5 and 8 λ_{D_i}. Tsytovich et al. (2008) have also pointed out that λ_g is usually close to the grain separation. Hence, only the first neighbour interaction is important and needs to be considered.

The necessity for the existence of an attractive inter-gain potential was pointed out (or at least emphasized) by Tsytovich (1994), who later reviewed (Tsytovich 1997) the state of knowledge in the subject, in particular the effect of shadowing of the flux of ions (Ignatov 1996; Khodataev et al. 1996; Tsytovich et al. 1996) and neutral species (Morfill et al. 1996) on a grain by another grain in the vicinity; the shadowing of the neutral particle flux (Morfill et al. 1996) may lead to an attractive or repulsive term. Finite stream of ion flux (Nambu et al. 1995; Shukla and Rao 1996; Vladimirov and Nambu 1996) in plasmas is considered to be responsible for this attractive potential between dust particulates with similar polarity on account of collective interactions involving ion oscillations in the flow. It is seen that the electrical potential due to the three shadowing processes is proportional to r^{-1}. Although expressions for the coefficients corresponding to different shadowing processes in the electric potential are available, it is pragmatic to lump these together as $(-A/r)$ and determine the value of A from the equilibrium inter-grain distance. Since these effects are caused only by grains in the vicinity, it is justifiable to take only the nearest neighbouring grains into consideration.

Thus, the attractive part of the inter-grain potential may be expressed as

$$\varphi_A(r) = -(A/r),$$

where A is a constant to be determined from the equilibrium inter-grain lattice parameter.

Resendes et al. (1998) concluded that the consideration of the overlap of Debye spheres of neighbouring grains leads to an attractive interaction energy $\varphi'_A(r)$ given by

$$\varphi'_A(r) = -\left(Z_d^2 e^2/2\lambda\right)\exp(-r/\lambda). \tag{3}$$

Some of the recent studies (Tskhakaya and Shukla 2004; Ivlev et al. 2008) suggest phenomena analogous to the van-der Waals attractive interaction potential where the dipole–dipole interactions of the compound dust particle can have an attractive behaviour. This dipole–dipole interaction term corresponding to an attractive potential may be expressed as

$$\varphi''_A(r) = -Z_d^2 e^2 \mu\left(\lambda^2/r^3\right), \tag{4}$$

where μ is a complex function of the incident angle and velocity of the ion and should be positive; this may be treated as constant in the context of the present study; the value of μ may be determined from the equilibrium lattice parameter.

Hence, in the present paper, the following four expressions for the inter-grain interaction energy have been considered:

$$\varphi(r) = \varphi_R(r) + \varphi_A(r) = \left[\left(Z_d^2 e^2/r\right)\exp(-r/\lambda)\right] - (A/r), \quad \text{(Yukawa, Shadow)} \tag{5}$$

$$\varphi(r) = \varphi'_R(r) + \varphi_A(r) = \left[\left(Z_d^2 e^2/r\right)(1 - r/\lambda_g)^4\right] - (A/r), \quad \text{(Gurevich, Shadow)} \tag{6}$$

$$\varphi(r) = \varphi_R(r) + \varphi'_A(r) = \left[\left(Z_d^2 e^2/r\right)\exp(-r/\lambda)\right] - \left(Z_d^2 e^2/2\lambda\right)\exp(-r/\lambda), \quad \text{(Yukawa, Resendes)} \tag{7}$$

$$\varphi(r) = \varphi_R(r) + \varphi''_A(r) = \left[\left(Z_d^2 e^2/r\right)exp(-r/\lambda)\right] - Z_d^2 e^2 \mu(\lambda^2/r^3). \quad \text{(Yukawa, Dipole)} \tag{8}$$

Equation (5) has been used by Amiranashvili et al. (2001) for the study of spectral properties of clusters of grains; however, λ was not considered as a function of λ_{Di} and β. The total interaction potential for a grain is of a simple form for crystalline structures in a complex plasma due to the short range of the interaction potential as compared to the lattice parameter in solids; one has thus to consider interactions between the nearest and the next nearest neighbours only.

Melandso (1996) has analysed the lattice vibrations of the simplest periodic structure, viz. the linear chain, using solid state theory, and derived the dispersion relations (ω vs k), where ω is the lattice vibration frequency, corresponding to the wavenumber $k$of the lattice wave propagating along the chain. However, he derived this

https://doi.org/10.1017/S0022377812000694 Published online by Cambridge University Press

relation based only on the Yukawa potential which is repulsive in nature and cannot ensure the equilibrium of the lattice. He assumed that the contribution of an additional attraction term in the potential energy for ensuring equilibrium is insignificant and can be ignored. However, for studies on periodic structures and lattice waves, it is not the magnitude of the potential but its first and second derivatives with respect to r which are important. Hence, ignoring attractive terms is not justified. Furthermore, Melandso (1996) based his analysis on the Green's function technique used in solid state theory in many situations but it is not common in conventional lattice vibrational studies.

In this paper, we have used the conventional methods of lattice dynamics (e.g. those described in Born and Huang 1994), to derive the dispersion relations for lattice waves in a linear chain and in 2D square and hexagonal lattices. A suitable lattice potential and Newton's second law of motion have been employed as compared to the relatively intricate method, based on the use of Green's function (Melandso 1996). For the Debye–Hückel interaction as the sole interaction between the grains, the results of the two approaches are in agreement.

2. Analysis

2.1. Lattice vibrations: Linear chain

Consider a long portion of an infinitely long chain with grains of equal charge $-Z_d e$ and mass m, having a period a in the equilibrium configuration. We number the grains with integer indices $\ldots j \ldots l \ldots$so that the equilibrium position of the jth grain from a chosen origin numbered zero can be written as ja. When the lattice executes small longitudinal oscillations, the position r_j of the jth grain changes from ja to $(ja + u_j)$ where u_j is the small displacement of the jth grain along the length of the chain such that $u_j \ll a$. The lattice potential (Φ_L) may be assumed to be made up of the total sum of all the pairwise central interaction potentials and therefore will be a function of all pairwise scalar separations (r_{jl}) between the jth and lth grains such as $r_{jl}(= |r_j - r_l|)$. The lattice potential can be written as

$$\Phi_L = (1/2) \sum_j \sum_{l \neq j} \varphi_{jl}(r_{jl}), \tag{9}$$

where φ_{jl} is the potential energy of the pair of grains j and l; the multiplier (1/2) appears because the lattice potential between grains j and l is counted twice in the sum as φ_{jl} and φ_{lj}.

This potential can be expanded in powers of small relative displacements $u_{jl}(= |u_l - u_j|)$. In the harmonic approximation, the expansion is taken only up to the square term in u_{jl}; thus, one can write

$$\Phi_L = \Phi_{L0} + \Phi_{L1} + \Phi_{L2},$$

where Φ_{L0} is the potential in the equilibrium configuration and hence a constant, Φ_{L1} is the term containing $(\partial \varphi_{jl}/\partial r_{jl})_0$ the subscript 0 outside the bracket indicating evaluation in the equilibrium state. This term must vanish since the net force acting on every grain in the equilibrium configuration of the unstrained lattice must be zero. Thus, the only relevant term in the expansion is

$$\Phi_{L2} = (1/4) \sum_j \sum_l \left[\partial^2 \varphi_{jl}/\partial r_{jl}^2\right]_0 u_{jl}^2. \tag{10}$$

The restriction $l \neq j$ has been dropped as the term will anyway vanish in view of $(u_{jl})_{j=l} = 0$. With the help of an invariance relation (i.e. $\sum_j [\partial^2 \varphi_j/\partial r_j^2]_0 = 0$), satisfied by a linear chain (Born and Huang 1994), (10) can be expressed better as

$$\Phi_{L2} = -(1/2) \sum_j \sum_l \left[\partial^2 \varphi_{jl}/\partial r_{jl}^2\right]_0 u_j u_l. \tag{11}$$

The equation of motion of the jth grain can now be expressed as

$$m\ddot{u}_j = -(\partial \Phi_L/\partial u_j) = -(\partial \Phi_{L2}/\partial u_j) = \sum_l \left[\partial^2 \varphi_{jl}/\partial r_{jl}^2\right]_0 u_l.$$

where l runs over all the grains and each dot overhead a variable indicates differentiation with respect to time. Since φ_{jl} depends only on the scalar distance r_{jl}, the index l could be ascribed to different grains counting 0 at the jth grain so that we can put the index $j = 0$, drop it in the sum on the right-hand side and write

$$m\ddot{u}_0 = \sum_l \left[\partial^2 \varphi_l/\partial r_l^2\right]_0 u_l. \tag{12}$$

One seeks a plane wave solution of (12) as

$$u_l = U \exp[i(\omega t - k r_{l0})] \quad \text{or} \quad u_l = U \exp[i(\omega t - kla)], \tag{13}$$

where r_{l0} represents the equilibrium position of the lth grain and is equal to la.

The periodic boundary condition may appear to be an artificial condition but is mathematically an effective one for a large aggregate of symmetrically arranged atoms and is therefore applicable to the grains in complex plasmas. It assumes dividing the entire aggregate in large identical blocks, each still containing a very large number of grains and that similarly located grains in various blocks oscillate in the same phase. Hence, for example in a linear chain if a block contains N grains, then the $(N+1)$th grain will belong to the next block. In this case, the phase of vibration of the first grain of the chosen block will always be the same as that of the $(N+1)$th grain so that

$$\exp(i\omega t) = \exp[i(\omega t - kNa)].$$

This demands

$$k = 2n\pi/Na, \tag{14}$$

where n is an integer running from 0 to N. Beyond N the integer n simply yields k values which repeat themselves. Thus, k is limited between 0 and $(2\pi/a)$. This range of k values defines the first Brillouin zone, which in view

https://doi.org/10.1017/S0022377812000694 Published online by Cambridge University Press

of symmetry, can be chosen to be from $(-\pi/a)$ to (π/a) instead of from 0 to $(2\pi/a)$.

The number of distinct allowed k values in the first Brillouin zone is just equal to the number of grains (or atoms) in the large block chosen in the boundary condition. In solids, this choice has helped in reducing the calculations as one could very well choose smaller number of k values according to convenience and necessity, particularly because in general the operative potentials do not quickly converge. In the case of complex plasmas, one finds that the potential is always fast converging and one can therefore obtain an analytical expression for the lattice vibration frequencies. One is therefore able to directly plot the dispersion relation curves as ω varying continuously with k.

Substituting u_l from (13) in (12), for non-zero U one obtains

$$m\omega^2 = \sum_l \left[\partial^2\varphi_l/\partial r_l^2\right]_0 \exp[-ikla]. \tag{15}$$

If we can write φ_l as an analytical function of r, the dispersion relation (ω vs k) can be obtained by using (15).

2.2. Analysis with the Yukawa and the attractive potential [equation (5)]

If the separation periodicity is r, one can write the repulsive potential energy of a single grain at the origin as

$$\varphi_R(r) = \sum_l \left(Z_d^2e^2/lr\right)\exp(-lr/\lambda). \tag{16}$$

In deriving the dispersion curves, however, the interactions have been chosen to act only up to (i) the nearest and (ii) the second nearest neighbours assuming the potential to decay fast, as done by Melandso (1996). For consistency, we have considered the equilibrium of the lattice (1) with both the repulsive and attractive potentials limited to the nearest neighbours and (2) the repulsive potential extending up to the second neighbours and attractive only limited to nearest ones as explained earlier; it may be noted that in the derivation of the ω vs k relation the same approximations have been used. This requires the expressions for A to differ in the two cases. Hence, we write:

Case 1: Both the repulsive and attractive potentials coupling only *nearest neighbours* (*NN*):

$$[\varphi(r)]_{NN} = \sum_{NN}\left\{\left(Z_d^2e^2/r\right)\exp(-r/\lambda) - (A_1/r)\right\}. \tag{17a}$$

Case 2: Repulsive potential extended to *next nearest neighbours* (*NNN*):

$$[\varphi(r)]_{NNN} = \sum_{NN}\left\{\left(Z_d^2e^2/r\right)\exp(-r/\lambda) - (A_2/r)\right\} + \sum_{NNN}\left(Z_d^2e^2/2r\right)\exp(-2r/\lambda). \tag{17b}$$

For the lattice to be in equilibrium (i.e. at $r = a$), one must have $[d\varphi(r)/dr]_{r=a} = 0$; this condition leads to

$$A_1 = Z_d^2e^2(1+\kappa)\exp(-\kappa). \quad \text{(Case 1)} \tag{18a}$$

$$A_2 = Z_d^2e^2[(\kappa+1)\exp(-\kappa) + (\kappa+1/2)\exp(-2\kappa)]. \quad \text{(Case 2)} \tag{18b}$$

These expressions are uniquely defined for a given value of $\kappa(= a/\lambda)$ and lead towards a stable configuration [i.e. $\varphi(r) < 0$] in the equilibrium ($r = a$); this can be readily seen by substituting for $A$from (18) into (17) at $r = a$.

2.3. The dispersion curves

The dispersion curves can now be directly obtained from (15) by using (17a) and (17b), with A_1 and A_2 given by (18a) and (18b). However, one has to take care of the periodicity of the lattice leading to the invariance relation [i.e. $\sum_j [\partial^2\varphi_j/\partial r_j^2]_0 = 0$], which defines the $j = 0$ term as

$$\frac{\partial^2\varphi_0}{\partial r_0^2} = -\sum_{l\neq 0}\left[\partial^2\varphi_l/\partial r_l^2\right]_0 = -\sum_{l\neq 0}\left[\partial^2(\varphi_{Rl}+\varphi_{Al})/\partial r_l^2\right]_0. \tag{19}$$

Substituting $(\varphi_R + \varphi_A)$ for φ in (15) and taking into consideration (5), the dispersion relation for the two cases may be written as

$$[\omega^2]_1 = \left(4Z_d^2e^2/ma^3\right)\left[(2+2\kappa+\kappa^2)\exp(-\kappa) - \{2(1+\kappa)\exp(-\kappa)\}\right]\sin^2(ka/2), \tag{20a}$$

$$[\omega^2]_2 = \left(4Z_d^2e^2/ma^3\right)[[(2+2\kappa+\kappa^2)\exp(-\kappa) - \{2(1+\kappa)\exp(-\kappa) + (1+2\kappa)exp(-2\kappa)\}] \times \sin^2(ka/2) + (1+2\kappa+2\kappa^2)\exp(-2\kappa)\sin^2 ka]. \tag{20b}$$

The expressions within the curly brackets in (20a) and (20b) represent the contributions of the attractive potential. The ratio (R) of the terms due to the attractive potential to that due the repulsive one [in (20a)] has been shown in Fig. 1(b) as a function of $\kappa(= a/\lambda)$. It is seen that the ratio is significant for moderate values of $\kappa(< 4)$. The rest in (20) is identical with the results of Melandso (1996).

2.4. The Gurevich screened and attractive potential [equation (6)]

In this case, $\varphi'_R(r) = (Z_d^2e^2/r)[1-(r/\lambda_g)]^4$ and $\varphi_A(r) = -(A/r)$.

For equilibrium at ($r = a$) using $[\partial(\varphi'_R + \varphi_A)/\partial r]_{r=a} = 0$, one obtains

$$A = \left(Z_d^2e^2/a\right)(1-a/\lambda_g)^3[1+(3a/\lambda_g)].$$

This leads the system to a stable configuration [$\varphi(r) < 0$] at equilibrium; this may be confirmed by substituting for A in (6) at $r = a$. Proceeding in the same way as before, remembering that $\varphi(r) = (\varphi'_R + \varphi_A)$ and limited

https://doi.org/10.1017/S0022377812000694 Published online by Cambridge University Press

in this case to the nearest neighbours, the dispersion relation obtained from (15) is seen to be

$$\omega^2 = \left(48Z_d^2e^2/ma\lambda_g^2\right)[1-(a/\lambda_g)]^2\sin^2(ka/2). \quad (21)$$

2.5. *Resendes potential including attractive term [equation (7)]*

The pair potential given by Resendes et al. (1998) *viz.* (7) can be expressed as

$$\varphi(r) = \left(Z_d^2e^2/r\right)[1-(r/2\lambda)]\exp(-r/\lambda). \quad (22)$$

The potential has no adjustable parameters and the equilibrium condition gives a fixed value of ($\kappa = a/\lambda$), viz. $\kappa = (\sqrt{3}+1)$, leaving the system in the stable configuration at equilibrium position (i.e. $\varphi(a) < 0$). This value of $\kappa(= a/\lambda)$ makes the second neighbour contribution to the lattice energy insignificant so that the lattice vibrations can be analysed on the basis of single-grain equilibrium.

Proceeding as in the other cases, one obtains the dispersion relation

$$\omega^2 = \left(16Z_d^2e^2/ma^3\right)(4+4\kappa+2\kappa^2-\kappa^3)\sin^2(ka/2). \quad (23)$$

Since the potential (7) gives a unique value for κ, this dispersion relation (ω vs k) is unique in contrast to the other dispersion relations, corresponding to a range of values of κ.

2.6. *Potential with dipole–dipole attraction term [equation (8)]*

Recalling (8), the pair potential in this case may be expressed as

$$\varphi(r) = \left(Z_d^2e^2/r\right)[\exp(-r/\lambda) - \mu(\lambda^2/r^2)]. \quad (24)$$

Again, in this case for a chosen value of the parameter $\mu(>0)$, the equilibrium position may be obtained by imposing the condition $(\partial\varphi/\partial r)_{r=a} = 0$, which yields $\kappa^2(1+\kappa)\exp(-\kappa) - 3\mu = 0$. This relation suggests two non-zero positive roots of κ for a given value of μ and restricts the span of μ within the range $0 < \mu < 0.61$; furthermore, the condition $(\partial^2\varphi/\partial r^2)_{r=a} > 0$ reveals the fact that the root $\kappa > (1+\sqrt{3})$ yields the system in stable equilibrium with minimum potential energy. Again, this value suppresses the contribution of *NNN* to the lattice potential energy and following the analysis as done in earlier sections, the dispersion relation may easily be derived as

$$\omega^2 = \left(4Z_d^2e^2/ma^3\right)[-(12\mu/\kappa^2) + (\kappa^2+2\kappa+2)\exp(-\kappa)] \times \sin^2(ka/2). \quad (25)$$

The expression for the dispersion relation in (25) reflects its uniqueness corresponding to a chosen value of the parameter $\mu(>0)$.

2.7. *Two-dimensional (plane) lattices*

Plane structures of grains in complex plasmas are only square and hexagonal (Khrapak et al. 2010). In the case of hexagon, choosing any grain as the origin 0 and an axis $-OX$ along the line joining a nearest neighbour (*NN*), one finds six *NN* grains at, say, a distance r located at the vertices of the hexagon with the centre at O and six next nearest neighbours (*NNN*) at a distance $r\sqrt{3}$, along the lines from the centre (origin) bisecting the six sides of the hexagon. In the simpler planar structure of the square lattice, the axes can be chosen along the sides. The potential coupling two grains will now be a function of two variables. We choose Cartesian coordinates (x, y) to represent the potential; the distance r can be written as $r(x, y)$. The Cartesian coordinates of the *NN* and *NNN* pairs in the equilibrium configuration for the two structures are given in Table 1.

Table 1. The *NN* and *NNN* grain coordinates for square and hexagonal structures (in equilibrium).

Nearness	Square	Hexagonal
NN	$(\pm a, 0), (0, \pm a)$	$(\pm a, 0), (\pm a\sqrt{3}/2, \pm a/2)$
NNN	$(\pm a\sqrt{2}, \pm a\sqrt{2})$	$(\pm 3a/2, \pm a\sqrt{3}/2), (0, \pm a\sqrt{3})$

The repulsive interaction potential can be expressed as φ_{R1} and φ_{R2} for the *NN* and *NNN* grains respectively and considered to be represented by the Yukawa potential. We further add to the repulsive potential an attractive potential $(-A/r)$ with a constant A, coupling only the nearest neighbours. Assuming the repulsive potential effective up to the second neighbours, the equilibrium condition yields the constant A in the two cases as

$$\text{Square}: \quad A = Z_d^2e^2\left[\exp(-\kappa) + (1/\sqrt{2})\exp(-\kappa\sqrt{2}) + \kappa\left\{\exp(-\kappa) + \exp(-\kappa\sqrt{2})\right\}\right], \quad (26)$$

$$\text{Hexagonal}: \quad A = Z_d^2e^2\left[\exp(-\kappa) + (1/\sqrt{3})\exp(-\kappa\sqrt{3}) + \kappa\left\{\exp(-\kappa) + \exp(-\kappa\sqrt{3})\right\}\right]. \quad (27)$$

Correspondingly, the equilibrium single-grain energy of the structures is negative for all $\kappa(= a/\lambda)$ values; this leads to the stability of the system.

2.8. *Small oscillations*

The small displacement **u** will now be indicated by (u_x, u_y) and (12) gets modified to

$$m\ddot{u}_\alpha(l) + \sum_j [\partial^2\varphi_{jl}/\partial r_j\partial r_l]_0 u_\beta(j) = 0, \quad (28)$$

where α and β take values 1 and 2 for x and y, respectively.

The plane wave solution can be expressed as

$$u_\alpha(l) = U(l)\exp\left[i(\omega t - \mathbf{k}\cdot\mathbf{r_0}(l)\right]. \quad (29)$$

Substitution of u_α from (29) into (28) yields a (2×2) determinantal equation for the evaluation of the normal mode frequencies, viz.

$$\begin{vmatrix} D_{11} - m\omega^2 & D_{12} \\ D_{21} & D_{22} - m\omega^2 \end{vmatrix} = 0, \quad (30)$$

https://doi.org/10.1017/S0022377812000694 Published online by Cambridge University Press

where $D_{\alpha\beta} = \sum_{NN} [\partial^2\varphi_{NN}/\partial x_\alpha \partial x_\beta]_0 \, [\exp[\mathbf{k}\cdot\mathbf{r_o}(NN)] - 1]$

$$+ \sum_{NNN} [\partial^2\varphi_{NNN}/\partial x_\alpha \partial x_\beta]_0 \, [\exp[\mathbf{k}\cdot\mathbf{r_o}(NNN)] - 1]. \quad (31)$$

An evaluation of $D_{\alpha\beta}$ from (31) and substitution in (30) leads to a relation between ω and $\mathbf{k}$. As an example, one may consider $D_{\alpha\beta}$ for (k_1, k_2) in a square lattice, a direct differentiation reveals

$$\left(\frac{\partial^2\varphi(r)}{\partial x_\alpha \partial x_\beta}\right) = \left(\frac{d^2\varphi(r)}{dr^2}\right)\left(\frac{x_\alpha x_\beta}{r^2}\right) + \left(\frac{d\varphi(r)}{rdr}\right)\left(\delta_{\alpha\beta} - \frac{x_\alpha x_\beta}{r^2}\right). \quad (32)$$

Using the notations $\alpha_1 = (\frac{d^2\varphi_{NN}(r)}{dr^2})$, $\beta_1 = (\frac{d\varphi_{NN}(r)}{rdr})$, $\alpha_2 = (\frac{d^2\varphi_{NNN}(r)}{dr^2})$ and $\beta_2 = (\frac{d\varphi_{NNN}(r)}{rdr})$, and substituting these parameters with $\mathbf{k} = (k_1, k_2)$ in (31), one gets

$$D_{11} = 4\alpha_1 \sin^2(k_1 a/2) + 4\beta_1 \sin^2(k_2 a/2) + 2(\alpha_2 + \beta_2) \times [\sin^2[(k_1 + k_2)a/2] + \sin^2[(k_1 - k_2)a/2]], \quad (33a)$$

$$D_{12} = D_{21} = 2(\alpha_2 - \beta_2)[\sin^2[(k_1 + k_2)a/2] + \sin^2[(k_1 - k_2)a/2]], \quad (33b)$$

and

$$D_{22} = 4\alpha_1 \sin^2(k_2 a/2) + 4\beta_1 \sin^2(k_1 a/2) + 2(\alpha_2 + \beta_2)\sin^2 \times [(k_1 + k_2)a/2] + \sin^2[(k_1 - k_2)a/2]. \quad (33c)$$

2.9. Square structures

In this model, $\varphi_{NN}(r)$ and $\varphi_{NNN}(r)$ can be written directly from the Yukawa potential extended up to the second neighbours and the attractive potential limited to the nearest neighbour so that the pair potentials

$$\varphi_{NN}(r) = \left(Z_d^2 e^2/r\right)\exp(-r/\lambda) - (A/r) \quad (34a)$$

and

$$\varphi_{NNN}(r\sqrt{2}) = \left(Z_d^2 e^2/r\sqrt{2}\right)\exp(-r\sqrt{2}/\lambda). \quad (34b)$$

Using the expression for A from (26), one obtains

$$\beta_1 = \left(Z_d^2 e^2/a^3\sqrt{2}\right)[\exp(-\kappa\sqrt{2})(1 + \kappa\sqrt{2})], \quad (35a)$$

$$\alpha_1 = \left(Z_d^2 e^2/a^3\sqrt{2}\right)[\kappa^2\exp(-\kappa) - 2\kappa\exp(-\kappa\sqrt{2}) - \sqrt{2}\exp(-\kappa\sqrt{2})], \quad (35b)$$

$$\beta_2 = -\left(Z_d^2 e^2/a^3\sqrt{2}\right)[(1 - \kappa\sqrt{2})\exp(-\kappa\sqrt{2})] \quad (35c)$$

and

$$\alpha_2 = \left(Z_d^2 e^2/a^3\sqrt{2}\right)[(2\kappa^2 + 2\sqrt{2}\kappa + 2)\exp(-\kappa\sqrt{2})]. \quad (35d)$$

One can now readily obtain ω for any chosen $\mathbf{k}$; however, one usually considers the dispersion relations in the symmetry directions only, e.g. $\mathbf{k} = (k, 0)$ and $\mathbf{k} = (k/\sqrt{2}, k/\sqrt{2})$; ω versus k for these symmetry directions have been evaluated and graphically illustrated.

Table 2. Relevant range of values of $\kappa(= a/\lambda)$.

Authors	Values of $\kappa(= a/\lambda)$
Thomas et al. (1994)	0.6−4.5
Homann et al. (1997)	0.6−4.5; 2.2 for maximum Z_d viz. 18 000
Nakamura and Ishihara (2009)	4.2 and ∼ 1 in a 2D case
Yaroshenko et al. (2005)	1.2−3.0
Antonova et al. (2008)	6.7
Peters et al. (1996)	1.5−3.0

2.10. Hexagonal structures

In this case, we have

$$\varphi_{NN}(r) = \left(Z_d^2 e^2/r\right)[\exp(-r/\lambda) - (1 + \kappa)\exp(-\kappa) - (1 + 1/\sqrt{3})\exp(-\kappa\sqrt{3})] \quad (36a)$$

and

$$\varphi_{NNN}(r) = \left(Z_d^2 e^2/r\sqrt{3}\right)\exp(-r\sqrt{3}/\lambda). \quad (36b)$$

Proceeding as in the case of a square, one obtains

$$\beta_1 = \left(Z_d^2 e^2/a^3\sqrt{3}\right)(1 + \kappa\sqrt{3})\exp(-\kappa\sqrt{3}), \quad (37a)$$

$$\alpha_1 = \left(Z_d^2 e^2/a^3\right)[\kappa^2\exp(-\kappa) - (2/\sqrt{3})(1 + \kappa\sqrt{3})\exp(-\kappa\sqrt{3})], \quad (37b)$$

$$\beta_2 = -\left(Z_d^2 e^2/3a^3\right)(1 - \kappa\sqrt{3})\exp(-\kappa\sqrt{3})] \quad (37c)$$

and

$$\alpha_2 = \left(Z_d^2 e^2/a^3\sqrt{3}\right)(3\kappa^2 + 2\sqrt{3}\kappa + 2)\exp(-\kappa\sqrt{3})]. \quad (37d)$$

These relations allow the dispersion curves to be obtained in symmetry directions, viz. $\mathbf{k} = (k, 0)$ and $\mathbf{k} = (k\sqrt{3}/2, k/2)$.

3. Numerical results and discussion

In models with the Yukawa and Gurevich screening, the expression for ω as a function of k contains a parameter $\kappa(= a/\lambda)$ or (a/λ_g), which can have a range of values (rather narrow) determined by the plasma parameters while the Resendes et al. (1998) potential corresponds to a unique value of κ. The single value or a range of values of κ, derived theoretically or measured, reported in the literature are listed in Table 2.

In general, it is believed that κ must be greater than unity for a periodic assembly of grains. Furthermore, as already mentioned, the Resendes potential (Resendes et al. 1998) corresponds to $\kappa = (\sqrt{3} + 1)$. In view of Table 2, three values of κ, viz. 2, 3 and 4, have been chosen for computations, corresponding to the models based on the Yukawa and Gurevich screening (λ_g has been chosen to be 5.5λ; Nefedov et al. 1998). The dispersion curves for these values of $\kappa(= a/\lambda)$ and (a/λ_g) have

https://doi.org/10.1017/S0022377812000694 Published online by Cambridge University Press

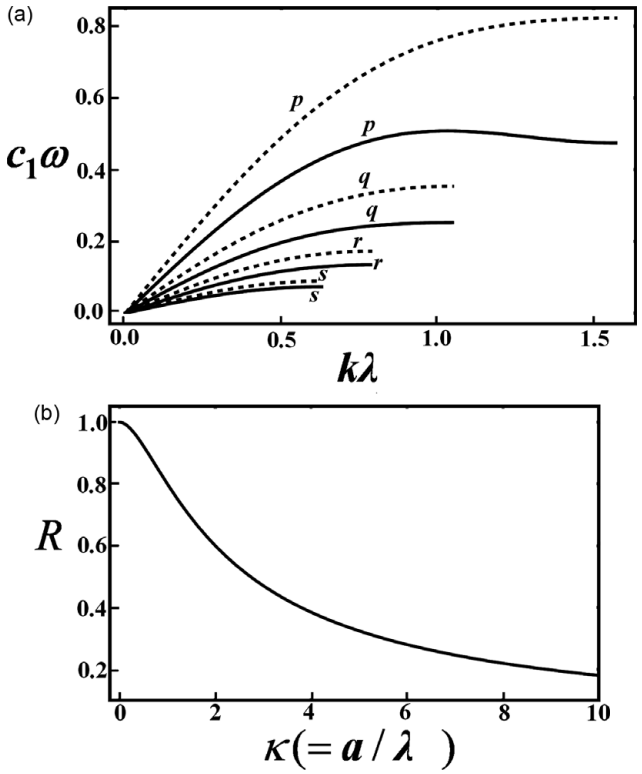


Figure 1. (a) Dispersion curves ($c_1\omega$ vs $k\lambda$) for the linear chain as a function of $\kappa(=a/\lambda)$. The labels *p, q, r* and *s* correspond to $\kappa = 2, 3, 4$ and 5, respectively, while the solid and broken curves refer to the present theory and the Melandso theory, respectively; here $c_1 = \left[m\lambda^3/Z_d^2e^2\right]^{1/2}$. (b) The ratio of the attractive to repulsive terms (R) in (20), contributing to the lattice wave frequency as a function of $\kappa(=a/\lambda)$.

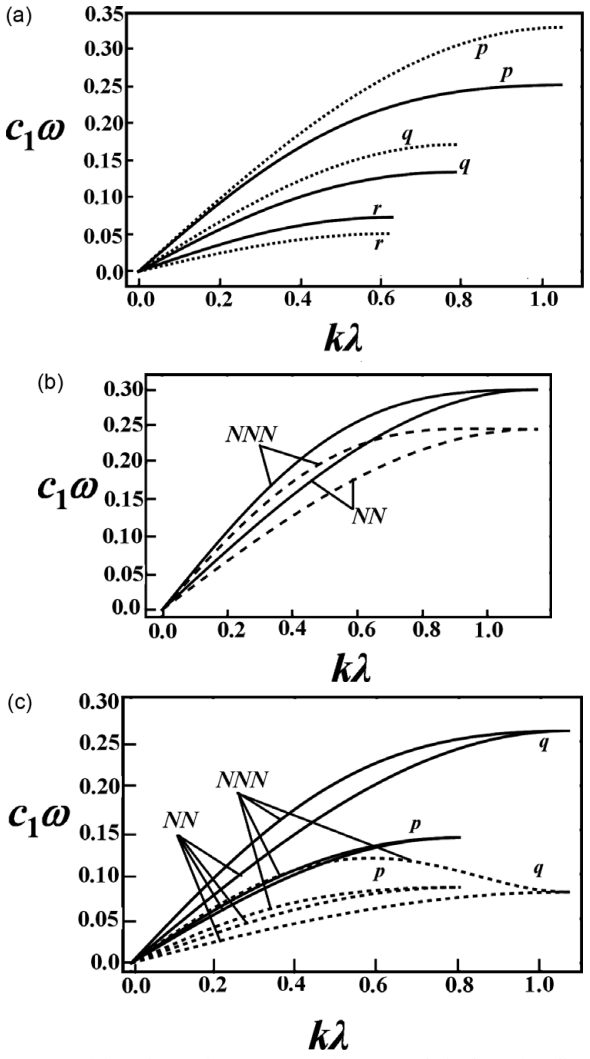


Figure 2. (a) Dispersion curves ($c_1\omega$ vs $k\lambda$) for the linear chain as a function of $\kappa(=a/\lambda)$. The labels *p, q* and *r* and correspond to $\kappa = 2, 3, 4$ respectively, while the solid and broken curves refer to the Debye and Gurevich screening, respectively. (b) Dispersion curve ($c_1\omega$ vs $k\lambda$) for the linear chain with $\kappa = (\sqrt{3}+1)$. The labels *NN and NNN* indicate that the interactions are limited up to the nearest and next nearest neighbours, respectively, while the solid and broken curves correspond to potentials used in the present and Resendes (1998) formulations, respectively. (c) Dispersion curve ($c_1\omega$ vs $k\lambda$) for the linear chain as a function of μ. The labels *p* and *q* correspond to $\kappa = 0.5$ and 0.6, respectively, while the labels *NN and NNN* are the same as in panel (b). The solid and broken curves correspond to potentials used in the present and Tskhakaya (Tskhakaya and Shukla 2004) formulations, respectively.

been obtained from (20)–(26). The Gurevich screening has been used only for the linear chain; the potential considering only the nearest neighbours was taken into account in this case because of the negligibility of the next-neighbour terms. The $\omega - k$ curves have been plotted for $0 < ka < \pi$ or $0 < k\lambda < (\pi/\kappa)$, where $\kappa = a/\lambda$. The set of Figs. 1 and 2 corresponds to a linear (1D) lattice while the set of Figs. 3 and 4 refers to the square and hexagonal (2D) lattices, respectively.

Figure 1(a) displays the dispersion curve in accordance with (i) the Melandso model (which considers only the screened Debye potential) and (ii) the authors' model, which takes into account both the repulsive potential and an attractive potential as discussed above. It is seen that the curves are significantly different for small values of κ $(= a/\lambda)$. The two sets of curves tend to converge for large values of $\kappa(> 5)$ [Fig. 1(b)] because the ratio of the terms in (20a), arising from the attractive and repulsive potentials, decreases with increasing κ. It may be remarked that it is this ratio and not the ratio of attractive to repulsive potentials (as considered by Melandso as a justification for neglecting the attractive potential), which is really important.

Figure 2(a) illustrates the dispersion curves, considering (i) the Debye screening and (ii) the Gurevich screening. It is seen that the nature of the screening has little effect on the dispersion curves; the effects decrease with increasing κ. Figure 2(b) displays the dispersion curves for the attractive potentials (i) $(-A/r)$ used in this paper and (ii) the attractive potential (Resendes et al. 1998) on account of overlapping Debye spheres for $\kappa = (\sqrt{3}+1)$; the contribution of *NN* and *NNN* for all the three cases has been displayed. Figure 2(c) shows a comparison of the Tskhakaya and Shukla (2004) formulation of attractive potential corresponding to a

https://doi.org/10.1017/S0022377812000694 Published online by Cambridge University Press

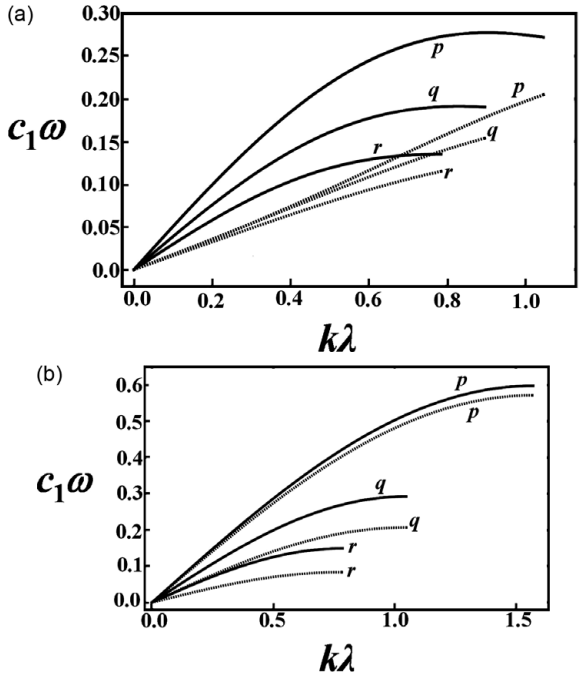


Figure 3. (a) Dispersion curves ($c_1\omega$ vs $k\lambda$) for a square lattice along the symmetric direction $\mathbf{k} = (k/\sqrt{2}, k/\sqrt{2})$ as a function of $\kappa(= a/\lambda)$. The labels p, q and r correspond to $\kappa = 3, 3.5$ and 4 respectively, while the solid and broken curves refer to the longitudinal and transverse modes respectively. (b) Dispersion curves ($c_1\omega$ vs $k\lambda$) for a square lattice along the symmetry direction $\mathbf{k} = (k, 0)$ as a function of $\kappa(= a/\lambda_D)$. The labels p, q and r correspond to $\kappa = 2, 3$ and 4 respectively, while the solid and broken curves are the same as in panel (a).

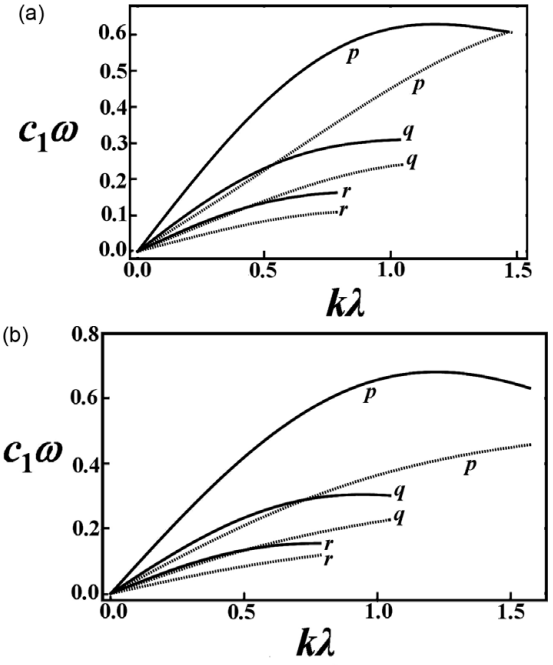


Figure 4. Dispersion curves ($c_1\omega$ vs $k\lambda$) for a hexagonal lattice along the symmetry direction (a) $\mathbf{k} = (k\sqrt{3}/2, k/2)$ and (b) $\mathbf{k} = (k, 0)$ as a function of $\kappa(= a/\lambda)$. In both panels, the labels p, q and r correspond to $\kappa = 2, 3$ and 4 respectively, while the solid and broken curves refer to the longitudinal and transverse modes respectively.

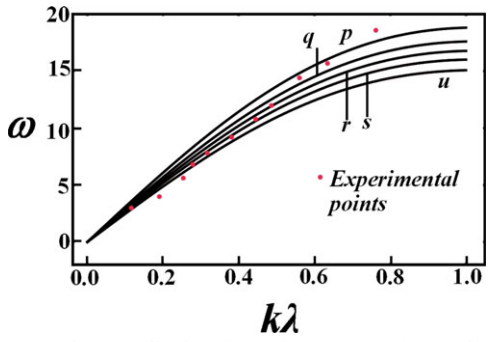


Figure 5. (Colour online) Dispersion curves (ω vs k) for the linear chain for the parameters $a = 930$ μm, $\rho = 1.514$ gcc^{-1}, $\kappa = 2.0$ and $Z_d = 18\,000$. The labels p, q, r, s and u correspond to $d = 8.8$, 9.2, 9.5, 9.8 and 10.2 μm, respectively. The solid curves correspond to the present theory while the dots refer to the experimental points given by Homann et al. (1997).

dipole–dipole interaction and presents an approach with attractive potential ($-A/r$) for different μ (or κ) values.

All the models, except that proposed by Resendes et al. (1998) and Tskhakaya and Shukla (2004), require an adjustable value of k to be determined by the experiment and hence the comparison of the computed dispersion curves with the experimental ones is not completely free of criticism. The model proposed by Resendes et al. (1998) and Tskhakaya and Shukla (2004) does not suffer from this handicap, but the agreement of the dispersion curves with experiments is not so good in this case.

The dispersion curves for a square lattice, corresponding to (i) the $\mathbf{k} = (k/\sqrt{2}, k/\sqrt{2})$ and (ii) $\mathbf{k} = (k, 0)$ directions, are displayed in Figs 3(a) and (b). It is interesting to observe that the curves for case (i) get nearer to each other as k increases while the reverse is true for case (ii). The curve corresponding to the longitudinal mode is always higher than those for the transverse mode. Figs 4(a) and (b) display the dispersion curves, corresponding to a hexagonal lattice structure for (i) $\mathbf{k} = (k\sqrt{3}/2, k/2)$ and (ii) $\mathbf{k} = (k, 0)$ directions. In both cases, the curves for longitudinal and transverse modes get closer with increasing values of κ. Homann et al. (1997) have experimentally obtained and graphically illustrated (their Fig. 5) a dispersion relation for lattice waves, corresponding to a linear chain with the following parameters: $a = 930$ μm, diameter of the particles $d = 2\Delta = (9.5 \pm 0.3)$ μm, density of the material of the particles $\rho = 1.514$ gcc^{-1}, $Z_d = (14\,000 \pm 4000)$ and $\kappa = (1 \pm 0.1)$, the parameter fitted to explain the observed curves on the basis of the Melandso (1996) theory. A good fit was obtained in the range $0 < k < 17$ cm^{-1}, in which the experiment was conducted; this corresponds to $0 < ka < 1.7$. The good fit of the relation, computed as per theory in this paper, to the experimental points is obtained and illustrated in Fig. 5 for the parameters given by Homann et al. (1997); the fitted value of the parameter κ is 2.0. It may be seen from the figure that the theoretical predictions in case of the linear chain are in agreement with experimental data. Note that the value $\kappa = (1 \pm 0.1)$, corresponding to the best fit as per

https://doi.org/10.1017/S0022377812000694 Published online by Cambridge University Press

the theory of Melandso (1996), is not in line with the value given in Table 2. Furthermore, recall that a theory solely based on a repulsive potential is not consistent with a lattice in equilibrium.

4. Conclusions

(1) It is interesting to note that the inter-grain potential energy model, proposed by Resendes et al. (1998), is inclusive of both repulsive and attractive terms and leads to a definite value of a/λ viz. $(\sqrt{3}+1)$ and hence a definite $\omega - k$ relation. This is in contrast to other models, which are used to arrive at an $\omega - k$ relation for different values of a/λ, and choose the one which gives best fit to the observed dispersion relation. Although the fit is certainly better for other models and for corresponding arbitrary values of a/λ, the model proposed by Resende et al. (1998) is conceptually better.

(2) It is seen that despite a low ratio of the magnitudes of the attractive to repulsive grain potentials, the contribution of the attractive potential to the dispersion relation is significant for moderate values of a/λ. This is on account of the importance of the second derivative of the potential in determining the dispersion relation.

(3) Theoretical results for the dispersion curve, corresponding to a linear chain, obtained on the basis of the Yukawa repulsive potential and a $1\backslash r$ attractive potential, are in good agreement with experiments (Homann et al. 1997) for a fitted value of a/λ. The present results are identical to those obtained by Melandso (1996), when the attractive potential is ignored.

Acknowledgements

The authors are grateful to the Department of Science and Technology, Government of India, for financial support and to Dr. Shikha Misra for helpful discussions.

References

Amiranashvili, Sh. G., Gusein-zade, N. G. and Tsytovich, V. N. 2001 *Phys. Rev.* E **64**, 016407.

Antonova, T., Annaratone, B. M., Thomas, H. M. and Morfill, G. E. 2008 *New J. Phys.* **10**, 043028.

Avinash, K., Khrapak, S. A. and Morfill, G. E. 2009 *Phys. Plasmas* **16**, 073706.

Baruah, S. and Das, N. 2010 *Phys. Plasmas* **17**, 073702.

Bin Liu, J. Goree, Fortov, V. E., Lipaev, A. M., Molotkov, V. I., Petrov, O. F., Morfill, G. E., Thomas, H. M., Rothermel, H. and Ivlev, A. V. 2009 *Phys. Plasmas* **16**, 083703.

Born, M. and Huang, K. 1994 *Dynamical Theory of Crystal Lattice*. London: Oxford University Press.

Bystrenko, I. O. and Zagardny, A. 1999 *Phys. Rev. Lett.* A **255**, 325.

Chaudhuri, M., Kompaneets, R. and Morfill, G. E. 2010 *Phys. Plasmas* **17**, 063705.

Chu, J. H. and Lin, I. 1994 *Phys. Rev. Lett.* **72**, 4009.

Couëdel, L., Nosenko, V., Zhdanov, S. K., Ivlev, A. V., Thomas, H. M. and Morfill, G. E. 2009 *Phys. Rev. Lett.* **103**, 215001.

Hayashi Y. and Tachibara K. 1994, *Jap. J. Appl. Phys.* **33**, L84.

Homann, A., Melzer, A., Peters, S. and Piel, A. 1997 *Phys. Rev.* E **56**, 7138.

Ignatov, A. M. 1996 *Plasma Phys.* **27**, 323.

Ikezi, H. 1986 *Phys. Fluids* **29**, 1764.

Ivlev, A. V. and Morfill, G. E. 2000 *Phys. Rev.* E **63**, 016409.

Ivlev A. V., et al. 2008 *Phys. Rev. Lett.* **100**, 095003.

Khodataev, Ya. K., et al. 1996 *Plasma Phys.* **27**, 125.

Khrapak, S. A. and Morfill, G. E. 2008 *Phys. Plasmas* **15**, 084502.

Khrapak, S. A., Ivlev, A. V., Morfill, G. E. and Thomas, H. 2002 *Phys. Rev.* E **66**, 046414.

Khrapak, S. A., Morfill, G. E., Ivlev, A. V., Thomas, H. M., Beysens, D. A., Zappoli, B., Fortov, V. E., Lipaev, A. M. and Molotkov, V. I. 2006 *Phys. Rev. Lett.* **96**, 015001.

Khrapak, S. A., Morfill, G. E., Fortov, V. E., Yachkov, L. G. D', Khrapak, A. G. and Petrov, O. F. 2007 *Phys. Rev. Lett.* **99**, 055003.

Khrapak, S. A., Ivlev, A. V. and Morfill, G. E. 2010 *Phys. Plasmas* **17**, 042107.

Klumov, B. A., Huber, P., Vladimirov, S., Thomas, H., Ivlev, A., Morfill, G. E., Fortov, V. E., Lipaev, A. and Molotkov, V. 2009 *Plasma Phys. Cont. Fusion* **51**, 124028.

Kompaneets, R., Konopka, U., Ivlev, A. V., Tsytovich, T. and Morfill, G. E. 2007 *Phys. Plasmas* **14**, 052108.

Knapek, C. A., Samsonov, D., Zhdanov, S., Konopka, U. and Morfill, G. E., 2007 *Phys. Rev. Lett.* **98**, 015004.

Konopka, U., Morfill, G. E. and Ratke, L. 2000 *Phys. Rev. Lett.* **84**, 891.

Lampe, M., Joyee, G. and Ganguli, G. 2000 *Phys. Plasmas* **7**, 3851.

Lampe, M., Goswami, R. and Sternovsky, Z. 2003 *Phys. Plasmas* **10**, 1500.

Maraduddin, A. A., Montroll, E. W., Weiss, G. H. and Ipatova, I. P. 1971 *Solid State Physics*, Supplement Three. London: Academic Press.

Melandso, F. 1996 *Phys. Plasmas* **3**, 3890.

Melandso, F. 1997 *Phys. Rev.* E **55**, 7495.

Melzer, A., Tottenberg, T. and Piel, A. 1994 *Phys. Lett.* A **191**, 301.

Misawa, T., Ohno, N., Asano, K., Sawai, M., Takamura, S. and Kaw, P. K. 2001 *Phys. Rev. Lett.* **86**, 1219.

Mitie, S., Klumov, B. A., Konopka, U., Thoma, M. H. and Morfill, G. E. 2008 *Phys. Rev. Lett.* **101**, 125002.

Morfill, G. E. and Ivlev, A. V. 2009, *Rev. Mod. Phys.* **81**, 1353.

Morfill, G. E., Khodataev, Ya. K. and Tsytovich, V. N., 1996 *Comments Plasma Phys. Contr. Fusion* **17**, 342.

Nefedov, A. P., Petrov, O. F. and Khrapak, S. A. 1998 *Plasma Phys. Rep.* **24**, 1037.

Nakamura, Y. and Ishihara, O. 2009 *Phys. Plasmas* **16**, 043704.

Nambu, M., Vladimirov, S. V. and Shukla, P. K. 1995 *Phys. Lett.* A **203**, 40.

Peters, S., Homann, A., Meltzer, A. and Piel, A. 1996 *Phys. Lett.* A **223**, 389.

Pieper, J. B. and Goree, J. 1996 *Phys. Rev. Lett.* **77**, 3137.

Pramanik, J., Prasad, G., Sen, A. and Kaw, P. K. 2002 *Phys. Rev. Lett.* **88**, 175001.

https://doi.org/10.1017/S0022377812000694 Published online by Cambridge University Press

Quinn, R. A., Cui, C., Goree, J., Pieper, J. B., Thomas, H. and Morfill, G. E. 1996 *Phys. Rev.* E **53**, R2049.

Ratynskaia, S., de Angdio, U., Khrapak, S. A., Klumov, B. and Morfill, G. E. 2006 *Phys. Plasmas* **13**, 104508.

Resendes, D. P., Mendonca, J. T. and Shukla, P. K. 1998 *Phys. Lett*. A **239**, 181.

Sato, N., et al. 1994 *Phys. Plasmas* **1**, 3480.

Shukla, P. K. and Eliasson, B. 2009 *Rev. Mod. Phys.* **81**, 25.

Shukla, P. K. and Mamun, A. A. 2002, *Introduction to Dusty Plasma Physics*. Bristol: IOP.

Shukla, P. K. and Rao, N. N. 1996 *Phys. Plasmas* **3**, 1770.

Thomas, H., Morfill, G. E., Demmel, V., Goree, J., Feuerbacher, B. and Mohamann, D. 1994 *Phys. Rev. Lett*. **73**, 652.

Tskhakaya, D. D. and Shukla, P. K. 2004, *JETP* **98**, 53.

Tsytovich, V. N., 1994 *Comments Plasma Phys. Contr. Fusion* **15**, 349.

Tsytovich, V. N. 1997 *Phys. Uspekhi* **40**, 53.

Tsytovich, V. N., Khodataev, Ya. K., Bingham, R. 1996 *Comments Plasma Phys. Contr. Fusion* **17**, 221.

Tsytovich, V. N., Gusei-zade, N. and Morfill, G. April 2004 *IEEE Trans. Sci. Special Issue Dusty Plasmas* **32**, 637.

Tsytovich, V. N., Morfill, G. E., Vladimirov, S. V. and Thomas, H. 2008 *Elementary Physics of Complex Plasma*. Berlin: Springer.

Vladimirov, S. V. and Ishihara, O. 1996 *Phys. Plasmas* **3**, 444.

Vladimirov, S. V. and Nambu, M. 1996 *Phys. Rev.* E **52**, R2172.

Vladimirov, S. V., Shevechenko, P. V. and Cramer, N. F. 1997 *Phys. Rev.* E **56**, R74.

Vladimirov, S. V., Cramer, N. F. and Shevchenko, P. V. 1999 *Phys. Rev.* E **60**, 7369.

Vladimirov, S. V., Yaroshenko, V. V. and Morfill, G. E., 2006 *Phys. Plasmas* **13**, 030703.

Yaroshenko, V. V., Ivlev, A. V. and Morfill, G. E. 2005 *Phys. Rev.* E **71**, 046405.

https://doi.org/10.1017/S0022377812000694 Published online by Cambridge University Press